



Universiteit
Leiden
The Netherlands

Functional inhibition of host histone deacetylases (HDACs) enhances in vitro and in vivo anti-mycobacterial activity in human macrophages and in zebrafish

Moreira, J.D.; Koch, B.E.V.; Veen, S. van; Walburg, K.V.; Vrieling, F.; Pinto Dabés Guimarães, T.M.; ... ; Heemskerk, M.T.

Citation

Moreira, J. D., Koch, B. E. V., Veen, S. van, Walburg, K. V., Vrieling, F., Pinto Dabés Guimarães, T. M., ... Heemskerk, M. T. (2020). Functional inhibition of host histone deacetylases (HDACs) enhances in vitro and in vivo anti-mycobacterial activity in human macrophages and in zebrafish. *Frontiers In Immunology*, 11, 36.
doi:10.3389/fimmu.2020.00036

Version: Publisher's Version
License: [Creative Commons CC BY 4.0 license](https://creativecommons.org/licenses/by/4.0/)
Downloaded from: <https://hdl.handle.net/1887/3134674>

Note: To cite this publication please use the final published version (if applicable).



Functional Inhibition of Host Histone Deacetylases (HDACs) Enhances *in vitro* and *in vivo* Anti-mycobacterial Activity in Human Macrophages and in Zebrafish

OPEN ACCESS

Edited by:

Christoph Hölscher,
Research Center Borstel
(LG), Germany

Reviewed by:

Larry Schlesinger,
The Ohio State University,
United States

Ronan Kapetanovic,
University of Queensland, Australia

*Correspondence:

Mariëlle C. Haks
m.c.haks@lumc.nl

†These authors have contributed
equally to this work

‡ORCID:

Mariëlle C. Haks
orcid.org/0000-0002-7538-1800

Specialty section:

This article was submitted to
Microbial Immunology,
a section of the journal
Frontiers in Immunology

Received: 23 August 2019

Accepted: 08 January 2020

Published: 03 February 2020

Citation:

Moreira JD, Koch BEV, van Veen S,
Walburg KV, Vrieling F, Mara Pinto
Dabés Guimarães T, Meijer AH,
Spaink HP, Ottenhoff THM, Haks MC
and Heemsker MT (2020) Functional
Inhibition of Host Histone
Deacetylases (HDACs) Enhances
in vitro and *in vivo* Anti-mycobacterial
Activity in Human Macrophages and in
Zebrafish. *Front. Immunol.* 11:36.
doi: 10.3389/fimmu.2020.00036

Jôsimar D. Moreira^{1,2}, Bjørn E. V. Koch³, Suzanne van Veen¹, Kimberley V. Walburg¹, Frank Vrieling¹, Tânia Mara Pinto Dabés Guimarães², Annemarie H. Meijer³, Herman P. Spaink³, Tom H. M. Ottenhoff¹, Mariëlle C. Haks^{1*†‡} and Matthias T. Heemsker^{1†}

¹ Department of Infectious Diseases, Leiden University Medical Center, Leiden, Netherlands, ² Department of Clinical and Toxicological Analysis, Faculty of Pharmacy, Federal University of Minas Gerais, Belo Horizonte, Brazil, ³ Institute of Biology Leiden, Leiden University, Leiden, Netherlands

The rapid and persistent increase of drug-resistant *Mycobacterium tuberculosis* (*Mtb*) infections poses increasing global problems in combatting tuberculosis (TB), prompting for the development of alternative strategies including host-directed therapy (HDT). Since *Mtb* is an intracellular pathogen with a remarkable ability to manipulate host intracellular signaling pathways to escape from host defense, pharmacological reprogramming of the immune system represents a novel, potentially powerful therapeutic strategy that should be effective also against drug-resistant *Mtb*. Here, we found that host-pathogen interactions in *Mtb*-infected primary human macrophages affected host epigenetic features by modifying histone deacetylase (HDAC) transcriptomic levels. In addition, broad spectrum inhibition of HDACs enhanced the antimicrobial response of both pro-inflammatory macrophages (M ϕ 1) and anti-inflammatory macrophages (M ϕ 2), while selective inhibition of class IIa HDACs mainly decreased bacterial outgrowth in M ϕ 2. Moreover, chemical inhibition of HDAC activity during differentiation polarized macrophages into a more bactericidal phenotype with a concomitant decrease in the secretion levels of inflammatory cytokines. Importantly, *in vivo* chemical inhibition of HDAC activity in *Mycobacterium marinum*-infected zebrafish embryos, a well-characterized animal model for tuberculosis, significantly reduced mycobacterial burden, validating our *in vitro* findings in primary human macrophages. Collectively, these data identify HDACs as druggable host targets for HDT against intracellular *Mtb*.

Keywords: tuberculosis, host-directed therapy, epigenetic regulation, histone deacetylases (HDAC), human macrophages

INTRODUCTION

Tuberculosis (TB) is a health threat of global dimensions, and is caused by the highly successful human pathogen *Mycobacterium tuberculosis* (*Mtb*). Remarkably, *Mtb* is capable of establishing intracellular infection even in the presence of strong innate and adaptive host immunity. One fourth of the global human population is estimated to be latently infected with *Mtb*. These individuals have a 5–10% lifetime risk of developing TB reactivation disease, resulting in 10 million people falling ill with TB and over 1.5 million deaths each year (1). In HIV-infected or otherwise immunocompromised patients the risk of TB reactivation is significantly increased.

Current interventions (antibiotics, BCG vaccination) fail to reduce TB incidence sufficiently. Together with the rising frequency of multi-, extensively-, and even totally drug-resistant (MDR/XDR/TDR) *Mtb* strains, and the fact that many druggable targets in pathogens are already inhibited by current antibiotics (2), it is crucial to develop new and much more effective strategies that act by mechanisms different from those already targeted by current interventions. Since *Mtb* has a remarkable ability to manipulate intracellular signaling pathways which promote its escape from host defense in human cells, host-directed therapies (HDT) would represent a therapeutic strategy that would be effective also against currently untreatable strains since these compounds act on host and not on pathogen molecules.

TB most commonly presents as a pulmonary disease following inhalation of *Mtb*-containing droplets in the lung. Modulation of host signaling pathways by *Mtb* in infected alveolar macrophages arrests phagosome maturation to create a niche for its intracellular survival (3, 4). In addition, activation of alveolar macrophages results in transcriptional changes that regulate innate and adaptive immune responses such as production of chemokines and pro- and anti-inflammatory cytokines (5). Epigenetic regulators play a crucial role in regulating the transcriptional response to microorganisms by chromatin remodeling (6, 7). Acetylation of histone proteins is one of the main mechanisms to control DNA accessibility and thereby gene expression (8). Histone acetyltransferases (HATs) acetylate lysine residues in histone tails resulting in a more relaxed chromatin structure which is associated with transcriptional activation. In contrast, histone-deacetylases (HDACs) counteract the activity of HATs by removing acetyl groups from highly conserved lysine residues resulting in more condensed chromatin structure which is associated with transcriptional repression by limiting the accessibility to the transcriptional machinery. HDACs are divided into four classes: Class I (HDAC1, 2, 3, and 8), class II (class IIa HDAC4, 5, 7, and 9; class IIb HDAC6 and 10), class III (SIRT1–7), and class IV (HDAC11) based on their function, co-factor dependency and structural homology to yeast HDACs (9). Class I, II, and IV enzymes belong to the family of “classical” HDACs and have a zinc-dependent active site, whereas class III proteins are NAD⁺-dependent and considered a family of “non-classical” HDACs.

HDACs are important players in the differentiation of macrophages and their role in immunity. HDAC3 has been shown to be vital in the development of anti-inflammatory

macrophages (M ϕ 2) by repressing alternative macrophage activation (10) whereas pro-inflammatory macrophages (M ϕ 1) are impacted by several HDACs, such as HDAC4, 5, 6, and 7, which strongly regulate the expression of pro-inflammatory genes upon stimulation with e.g., lipopolysaccharide (LPS) (11–13). Granuloma formation in the lungs of TB infected individuals is driven by macrophages and the resulting outcome of infection, i.e., bacterial control or bacterial dissemination, relies on macrophage type, and polarization (14, 15). It is therefore not surprising that several pathogens, including *Mtb* have been implicated in evading the immune system by modulating histone acetylation via altering HDAC expression levels (11, 16–19).

In the present study, we investigated the expression kinetics of different classes of HDAC transcripts in response to *Mtb* infection in primary human macrophages and found expression levels of a diverse set of HDAC genes to be affected by *Mtb*. We next investigated the impact of HDAC inhibition on infection in human macrophages *in vitro*. A pan-HDAC inhibitor as well as several selective class IIa inhibitors significantly reduced outgrowth of intracellular *Mtb* in macrophages. Importantly, these results were validated in an *in vivo* model of tuberculosis, the *Mycobacterium marinum* (*Mmar*) zebrafish embryo infection model (20–22). Collectively these results establish the potential of HDAC inhibitors as novel host-directed therapeutics for TB.

MATERIALS AND METHODS

Reagents

H-89 dihydrochloride (PKA/PKB/AKT1 kinase inhibitor), 3-aminobenzoic acid ethyl ester (tricaine), and rifampicin were purchased from Sigma-Aldrich, Zwijndrecht, The Netherlands. H-89 analog 97i was synthesized by the Leiden Academic Center for Drug Research, Division of Medicinal Chemistry, Leiden University, Leiden, The Netherlands. Pan-HDAC inhibitor Trichostatin A (TSA) and class IIa HDAC inhibitors TMP195 and TMP269 were purchased from Selleckchem, Munich, Germany. Hygromycin B was acquired from Life Technologies-Invitrogen, Bleiswijk, The Netherlands. Recombinant human IFN- γ protein was acquired from R&D Systems, Wiesbaden, Germany.

Cell Culture

Peripheral blood mononuclear cells (PBMCs) were isolated from buffy coats obtained from healthy donors after written informed consent (Sanquin Blood Bank, Amsterdam, The Netherlands). Monocytes were isolated through density gradient centrifugation over Ficoll-Paque followed by CD14 MACS sorting (Miltenyi Biotec, Bergisch Gladbach, Germany) and differentiated for 6 days into pro-inflammatory (M ϕ 1) or anti-inflammatory (M ϕ 2) macrophages with 5 ng/ml of granulocyte-macrophage colony-stimulating factor (GM-CSF; Life Technologies-Invitrogen) or 50 ng/ml macrophage colony-stimulating factor (M-CSF; R&D Systems, Abingdon, UK), respectively, as previously reported (23). Cells were cultured at 37°C/5% CO₂ in Gibco Roswell Park Memorial Institute (RPMI) 1640 medium (Life Technologies-Invitrogen) supplemented with 10% FBS and 2 mM L-alanyl-L-glutamine (GlutaMAX) (PAA, Linz, Austria), 100 U/ml

penicillin, and 100 µg/ml streptomycin (Life Technologies-Invitrogen). Macrophage differentiation and activation status was determined by quantifying IL-12p40 and IL-10 secretion (for Mφ1 and Mφ2, respectively) by ELISA following stimulation of cells in the presence or absence of 100 ng/ml lipopolysaccharide (LPS) for 24 h (InvivoGen, San Diego, United States).

***Mtb* Infection of Macrophages**

Mtb [DsRed-expressing H37Rv (24)] was cultured in Difco Middlebrook 7H9 broth (Becton Dickinson, Breda, The Netherlands) supplemented with 10% ADC (Becton Dickinson) and 0.05% Tween 80 (Sigma-Aldrich). One day before infection, *Mtb* cultures were diluted to a density corresponding with early log-phase growth (OD₆₀₀ of 0.25). The following day, bacterial suspensions (or 7H9 for mock infections) were diluted in cell culture medium without antibiotics to reach a multiplicity of infection (MOI) of 10. MOI of the inoculum was verified by a standard colony-forming unit (CFU) assay. Cells seeded in 96-well flat-bottom plates at a density of 30,000 cells/well in appropriate cell culture medium without antibiotics 1 day prior to infection, were inoculated with 100 µl of the bacterial suspension, centrifuged for 3 min at 800 rpm, and incubated at 37°C/5% CO₂ for 60 min. Bacteria were then washed away with cell culture medium containing 30 µg/ml gentamicin sulfate (Lonza BioWhittaker, Basel, Switzerland), incubated for 10 min at 37°C/5% CO₂, followed by replacement with medium containing 5 µg/ml gentamicin sulfate and, if indicated, chemical compounds until readout by flow cytometry, Luminex, or CFU.

Chemical Compound Treatment

During differentiation, monocytes were treated for 6 days with 300 nM TMP195, 300 nM TMP269, 30 nM TSA, or DMSO at equal v/v (25). The 300 nM concentration used for TMP195 and TMP269 was based on results reported by Guerriero et al. (26) in a similar monocyte differentiation model and was not toxic. TSA was used at a concentration of 30 nM for 6 days because higher concentrations showed toxicity. Alternatively, *Mtb*-infected Mφ1 and Mφ2 were treated for 48 h with 10 µM TMP195, TMP269, H-89 and 97i, 100 nM TSA, or DMSO at equal v/v in medium containing 5 µg/ml gentamicin sulfate. Prior to these experiments, we had performed pilot experiments to exclude cellular toxicity on primary human macrophages. We found no toxicity for both TMP195 and TMP269 at 10 µM concentrations, which constitutes a standard concentration in initial drug screening, confirming results from Lobera et al. (25). Trichostatin A, however, was found to be highly toxic at 10 µM and was therefore evaluated at lower concentrations. A concentration of 0.1 µM was found to be non-toxic in our primary human macrophage model, agreeing well with previously published results (27).

Zebrafish Handling, Compound Treatment, and *Mycobacterium marinum* Infection

Zebrafish were handled in compliance with animal welfare regulations and maintained according to standard protocols (<http://zfin.org>). Fertilized embryos were maintained at 28°C and kept in egg water [60 µg/ml Instant Ocean Sea Salt

(Sera, Heinsberg Germany)]. Zebrafish embryos starting the 20 somite stage were exposed for the following 24 h to 10 µM TMP195, 30 nM TSA, or DMSO at equal v/v in egg water at 28°C. *Mycobacterium marinum* (*Mmar*) M-strain carrying a plasmid encoding the Wasabi fluorescent protein (28) was cultured in 7H9 medium with 10% BBL ADC enrichment medium (Becton Dickinson, Franklin Lakes, United States) and 50 µg/ml Hygromycin at 28°C, to an optical density OD₆₀₀ of ~1. For the duration of bacterial injections, zebrafish larvae were kept under anesthesia in egg water containing 0.02% buffered 3-aminobenzoic acid ethyl ester (tricaine) and infections were performed by microinjection of 250–300 CFU into the Duct of Cuvier at ~43 h post fertilization (hpf), 24 h post compound treatment, as previously described (29). At 3 days post infection (dpi), the infection was quantified by fluorescent pixel determination (30). Infected embryos were anesthetized using 0.02% tricaine in egg water and imaged using a Leica MZ16FA Fluorescence Stereo Microscope (Leica Microsystems, Wetzlar, Germany) equipped with a DFC420C color camera (Leica Microsystems, Wetzlar, Germany).

Colony-Forming Unit (CFU) Assay

CFU spot assays have been described elsewhere (31). Briefly, cells were lysed in H₂O containing 0.05% SDS. Cell lysates were serially diluted in multiple steps of 5-fold dilutions in 7H9 broth and 10 µl droplets were spotted onto square Middlebrook 7H10 agar plates and incubated for 12–14 days at 37°C. Bacterial colonies were enumerated using a microscope with a 2.5x magnification to enhance early detection of bacterial growth.

***Mtb* Growth Assay**

A volume of 100 µl of *Mtb* culture (OD₆₀₀ of 0.2) in 7H9 broth was plated in a flat-bottom 96-well plate containing 100 µl of 7H9 broth with TMP195, TMP269, TSA, or Rifampicin as a positive control or DMSO at equal v/v at indicated concentrations. Growth was evaluated at 37°C for 13 days and absorbance was measured by optical density at 550 nm on a Mithras LB 940 plate reader (Berthold Technologies, Bad Wildbad, Germany).

Flow Cytometry

Single cell suspensions were incubated for 5 min with 5% human serum (Sanquin Blood Bank) in PBS to block non-specific Fc-receptor binding, washed in PBS/0.1% BSA (Merck, Darmstadt, Germany) and stained with monoclonal antibodies against cell surface markers CD11b-PE, CD1a-BV605, CD80-FITC, CD86-AF700 (all BD BioSciences, Vianen, The Netherlands), CD14-FITC, and CD163-AF647 (BioLegend, San Diego, CA, USA) for 30 min at 4°C. Cells were washed twice in PBS/0.1% BSA and acquisition was performed using a BD FACSLyric™ Flow Cytometer (BD Biosciences). Data was analyzed using FlowJo v10 software.

Cell Viability Assay

Cells seeded at a density of 30,000 cells/well in 96-well flat-bottom plates were stained in 50 µl cell culture medium without phenol red containing propidium iodide (PI) (1:500, Sigma-Aldrich) and Hoechst (1:100, Sigma-Aldrich). After incubation for 5 min at

room temperature (RT), 3 images per well were recorded using a Leica AF6000 LC fluorescence microscope combined with a 20x dry objective. Cell viability was calculated by quantifying the number of dead cells (PI positive) vs. total cell numbers (Hoechst positive) using ImageJ software.

Microscopy

Bright field image acquisition was performed using an Olympus IX51 Inverted Microscope combined with Olympus cellSens software.

Cytokine and Chemokine Multiplex Beads Assay

Culture supernatants were collected 24 h post-infection and filter-sterilized by centrifugation in 96-well filter plates containing a 0.2 μ m PVDF membrane (Corning, Amsterdam, The Netherlands). Forty-one analytes were quantified using the Milliplex Human Cytokine/chemokine magnetic bead premixed 41-plex kit (Millipore Billerica, MA, USA) according to the manufacturer's instructions. Analyses were performed on a Bio-Plex 100 with Bio-Plex Manager™ software v6.1 (Biorad, Veenendaal, The Netherlands).

The following analytes were measured: sCD40L, EGF, FGF-2, Flt3 ligand, Fractalkine (CX3CL1), G-CSF, GM-CSF, GRO (CXCL1), IFN- γ , IFN- α 2, IL-1 α , IL-1 β , IL-1ra, IL-2, IL-3, IL-4, IL-5, IL-6, IL-7, IL-8 (CXCL8), IL-9, IL-10, IL-12p40, IL-12p70, IL-13, IL-15, IL-17a, IP-10 (CXCL10), MCP-1 (CCL2), MCP-3 (CCL7), MDC (CCL22), MIP-1 α (CCL3), MIP-1 β (CCL4), PDGF-AB/BB, RANTES (CCL5), TGF- α , TNF- α , TNF- β , VEGF, Eotaxin (CCL11), and PDGF-AA.

Phagocytosis Assay

Cells were pulsed with Fluoresbrite® YG Carboxylate Microspheres P beads (Polysciences, Warrington, PA, USA) in a ratio of 10 beads to 1 cell for 90 min at 37°C/5% CO₂. Cells were subsequently washed with PBS and harvested by adding Trypsin-EDTA 0.5% (ThermoFisher Scientific, Waltham, MA, USA). Cells were centrifuged and resuspended in 100 μ l Trypan Blue (1:1) in PBS/0.1% BSA (Merck) to quench fluorescence of extracellular beads. Internalized beads were quantified by flow cytometry on a BD FACSLyric™. Data analysis was performed using FlowJo v10 software.

Total RNA Isolation and cDNA Synthesis

Total RNA isolation was performed using TRIzol Reagent (Life Technologies-Invitrogen) according to the manufacturer's instructions and RNA yield was quantified using a DeNovix DS-11 Spectrophotometer (ThermoFisher Scientific). Total RNA (0.5 μ g) was reverse transcribed using SuperScript IV Reverse Transcriptase (Life Technologies-Invitrogen). Briefly, RNA samples were first incubated at 65°C for 5 min in the presence of 0.5 mM dNTPs and 2.5 μ M oligo(dT)₂₀ (Life Technologies-Invitrogen). Subsequently, cDNA synthesis was initiated by adding a master mix containing 1x first strand buffer, 5 mM DTT, 40 U RNaseOUT (ThermoFisher Scientific), and 200 U SuperScript IV and incubating at 50–55°C for 10 min followed by inactivation of the reverse transcriptase at 80°C for 10 min.

TaqMan qPCR

Multiplex quantitative polymerase chain reaction (qPCR) was carried out using a QuantStudio 6 Flex Real-Time PCR System (ThermoFisher Scientific). qPCR reactions were performed in a final volume of 25 μ l containing 1x TaqMan Universal PCR Master Mix, No AmpErase UNG, 1x HDAC(1-11)-FAM TaqMan primers (ThermoFisher Scientific), 0.5x GAPDH-VIC TaqMan primers (ThermoFisher Scientific), and 20 ng cDNA. Thermal cycling conditions were 1 cycle of 2 min/50°C and 10 min/95°C, followed by 60 cycles of 15s/95°C and 1 min/60°C. The threshold cycle (Ct) values of HDAC transcripts were normalized to GAPDH by the $2^{-\Delta\Delta CT}$ algorithm method (32). Relative expression levels were calculated by applying the formula $((2^{-\Delta CT(\text{Target gene})})/(2^{-\Delta CT(\text{GAPDH})}))$. The following TaqMan® Gene Expression Assays were used: GAPDH-VIC (Hs02758991_g1), HDAC1-FAM (Hs00606262_g1), HDAC2-FAM (Hs00231032_m1), HDAC3-FAM (Hs00187320_m1), HDAC4-FAM (Hs01041638_m1), HDAC5-FAM (Hs00608351_m1), HDAC6-FAM (Hs00997427_m1), HDAC7-FAM (Hs00248789_m1), HDAC8-FAM (Hs00954353_g1), HDAC9-FAM (Hs01081558_m1), HDAC10-FAM (Hs00368899_m1), HDAC11-FAM (Hs00978038_m1), TNF-FAM (Hs00174128_m1), IL6-FAM (Hs00174131_m1), CSF3-FAM (Hs00738432_g1), IFNG-FAM (Hs00989291_m1), CCL2-FAM (Hs00234140_m1), CCL3-FAM (Hs00234142_m1), CCL4-FAM (Hs99999148_m1), and CXCL8-FAM (Hs00174103_m1). TNF, IL6, CSF3, and IFNG could not be detected within a cycle threshold (Ct) of 45.

Data Analysis

Normal distribution of data sets was evaluated using the Shapiro-Wilk normality test. Paired sample *t*-test analysis was employed when comparing two experimental conditions. One-way ANOVA and repeated measure (RM) one-way ANOVA with Dunnett's multiple test correction were applied when assessing differences between 3 or more groups of unpaired and paired samples, respectively. Kruskal-Wallis test followed by Dunnett's multiple test correction was used when comparing non-parametric data sets of 3 or more groups. All analyses were performed using GraphPad Prism 8.

For multilevel partial least squares-discriminant analysis (PLS-DA) (33), the R package mixOmics (version 6.3.2) was used (34). Model validity was assessed by determining model quality characteristics for explained variance (R^2X , R^2Y) and predictive ability (Q^2_{cum}) after leave-one-out cross validation (LOOCV). Variable Importance in Projection (VIP) scores of the first *x*-variate, representing the contribution of each variable to the model, were extracted from each PLS-DA analysis and values ≥ 1 were considered relevant. Only analytes that changed in at least 3 out of 4 donors with a minimal median log₂ fold change (FC) of 0.5 were included in the analyses. The associations of analytes with treatment response are reflected by Kendall correlation coefficients. For calculation of the Kendall rank correlation coefficient tau-b, the R package Kendall (version 2.2) was used (35).

Fluorescent images of infected zebrafish embryos in Tiff file format were processed and quantified using the Fiji distribution of ImageJ (36). For the processing steps, involving

thresholding and quantification of positive pixels, an ImageJ macro was developed: run("8-bit"); setAutoThreshold("Triangle dark"); setThreshold(4, 255); run("Convert to Mask"); run("Measure"); close().

RESULTS

Regulation of HDAC Transcriptomic Profiles in Response to *Mtb* Infection

To explore whether intracellular survival of *Mtb* is controlled by host epigenetic features, we investigated whether *Mtb*-H37Rv (*Mtb*) infection could impact histone acetylation in primary human pro-inflammatory (M ϕ 1) and anti-inflammatory (M ϕ 2) macrophages (the main target cell of *Mtb*), representing opposing ends of the macrophage differentiation spectrum. Expression kinetics of all 11 canonical HDAC transcripts were determined in triplicate by qRT-PCR before (baseline) and 4 and 24 h following infection with *Mtb* (Figure 1). Differential regulation of HDAC transcript levels upon *Mtb* infection was more pronounced in M ϕ 2 than M ϕ 1. HDAC1 was substantially upregulated 24 h post-infection in both M ϕ 1 and M ϕ 2. In contrast, expression levels of HDAC3, 5, 7, 10, and 11 were significantly repressed in M ϕ 2 whereas in M ϕ 1 this was only observed for HDAC5. Interestingly, expression levels of 4 out of 5 HDACs that were significantly suppressed in M ϕ 2 following infection with *Mtb*, exhibited significantly higher transcript levels in M ϕ 2 compared to M ϕ 1 at baseline (Figure S1A). Since HDACs are considered molecular switches regulating a plethora of processes including balancing pro-vs. anti-inflammatory responses (Table 1), distinct baseline expression levels of HDAC family members might explain differences in inflammatory cytokine profiles between activated M ϕ 1 and M ϕ 2 (23). Using a published RNA-sequencing dataset of *Mtb*-infected M ϕ 2, we were able to independently validate our findings [markedly enhanced expression levels of HDAC1 and significantly reduced transcript levels of HDAC3, 5, 10, and 11 upon infection with *Mtb*-H37Rv, heat-killed *Mtb*-H37Rv and Bacillus Calmette-Guérin (BCG)] for anti-inflammatory macrophages (Figure S1B) (64). Interestingly, lower expression levels of HDAC3, 5, 10, and 11 were not seen at early timepoints after infection with *Mtb*-GC1237, a virulent Beijing strain, implying that this could be advantageous to the pathogen. This suggests that lowering these specific HDAC expression levels might be beneficial to the host. Together, these data suggest that host-pathogen interactions in *Mtb*-infected macrophages affect host epigenetic features by modifying histone acetylation through regulating HDAC expression levels. Therefore, targeting HDACs with small molecules could potentially regulate outgrowth of intracellular infections with *Mtb*.

Chemical Inhibition of HDACs Markedly Reduces Intracellular Survival of *Mtb*

To investigate whether histone acetylation/deacetylation controls *Mtb* infection, *Mtb*-infected M ϕ 1 and M ϕ 2 were treated with selective class IIa HDAC inhibitors [TMP195 and TMP269 (25)] or the pan-HDAC inhibitor Trichostatin A (TSA) (Figure 2A).

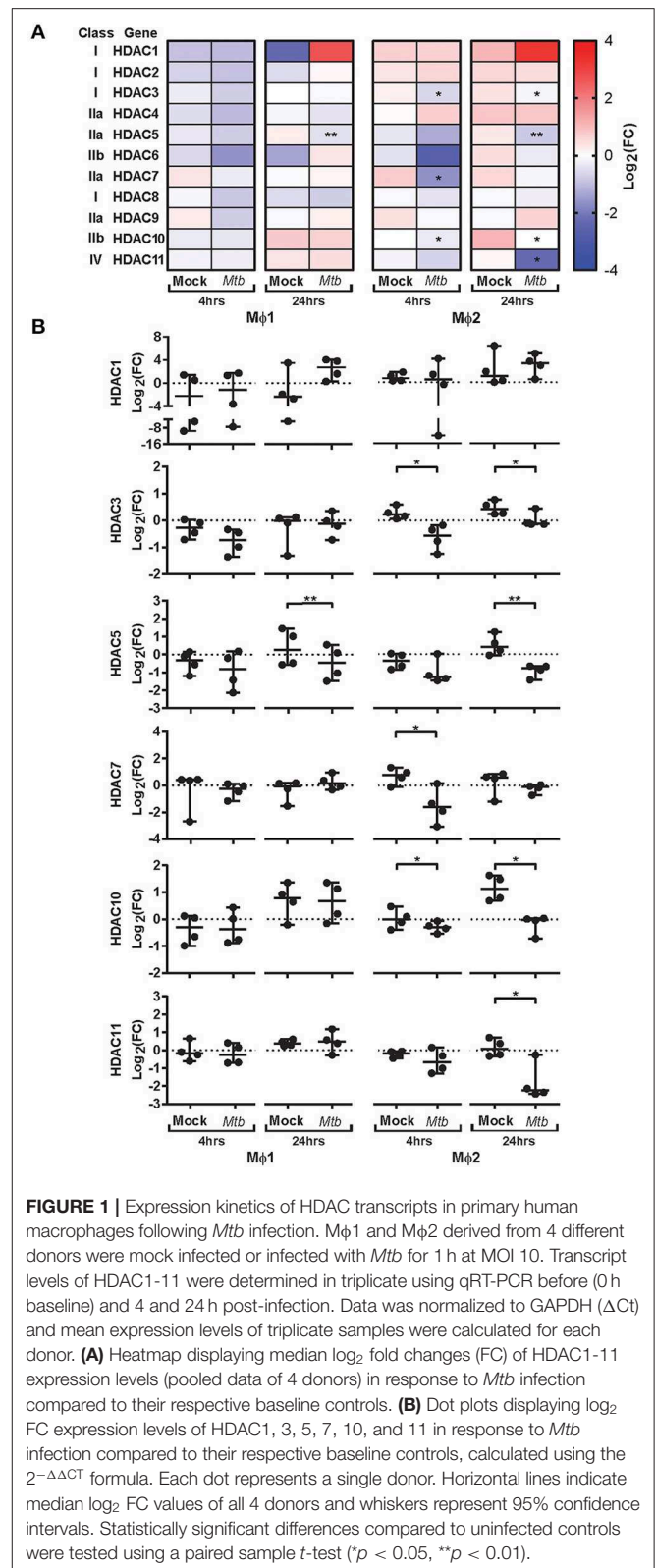


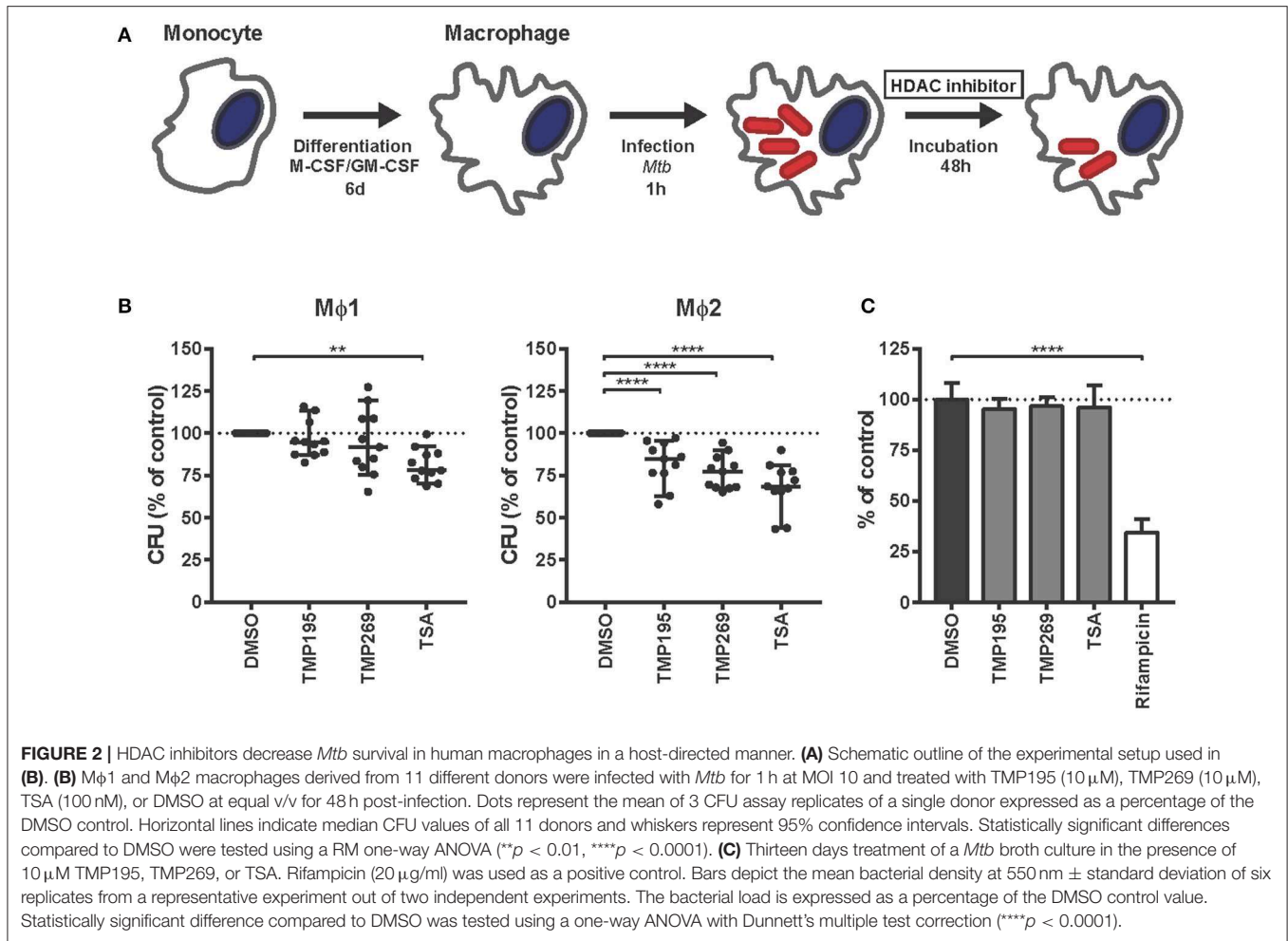
FIGURE 1 | Expression kinetics of HDAC transcripts in primary human macrophages following *Mtb* infection. M ϕ 1 and M ϕ 2 derived from 4 different donors were mock infected or infected with *Mtb* for 1 h at MOI 10. Transcript levels of HDAC1-11 were determined in triplicate using qRT-PCR before (0 h baseline) and 4 and 24 h post-infection. Data was normalized to GAPDH ($\Delta\Delta C_T$) and mean expression levels of triplicate samples were calculated for each donor. **(A)** Heatmap displaying median \log_2 fold changes (FC) of HDAC1-11 expression levels (pooled data of 4 donors) in response to *Mtb* infection compared to their respective baseline controls. **(B)** Dot plots displaying \log_2 FC expression levels of HDAC1, 3, 5, 7, 10, and 11 in response to *Mtb* infection compared to their respective baseline controls, calculated using the $2^{-\Delta\Delta C_T}$ formula. Each dot represents a single donor. Horizontal lines indicate median \log_2 FC values of all 4 donors and whiskers represent 95% confidence intervals. Statistically significant differences compared to uninfected controls were tested using a paired sample *t*-test (* $p < 0.05$, ** $p < 0.01$).

Given the nature and mechanisms of action of the HDAC targets (which enzymatically control epigenetic state), we hypothesized that a higher end dose of inhibitors was needed to be able

TABLE 1 | Regulation of cytokine/chemokine expression by HDACs in phagocytes.

Class	HDAC enzyme	Analyte	Immunostimulatory agent	Method of interference	Cell type	References
I	HDAC1	IL-1 β	LPS + IFN- γ	Genetic (siRNA)	RAW 264.7	(37)
		IL-12p40	<i>Mtb</i>	Genetic (siRNA)	THP-1	(18)
		IL-8	LPS	Genetic (siRNA)	GM-CSF differentiated human M ϕ	(38)
		IL-1 β , IL-10, IL12p40, TNF- α	LPS + IFN- γ	Chemical (MS-275)	RAW 264.7	(39)
		IL-1 β , IL-10	LPS	Chemical (MS-275)	RAW 264.7	(40)
		IL-6, IL-10, IL-12, TNF- α	poly(I:C)	Chemical (MS-275)	IL-4 + GM-CSF differentiated human DC	(41)
I	HDAC2	IL-1 β , IL-1ra	LPS	Chemical (Ky-2)	THP-1	(42)
		MIP-2 α , TNF- α	LPS	Genetic (overexpression)	RAW 264.7, PM ϕ	(43)
		IL-12p70, TNF- α	LPS	Chemical (Theophylline)	RAW 264.7, BMM ϕ	(44)
		IL-6	LPS	Genetic (siRNA)	IL-4 + GM-CSF differentiated BMDC	(45)
I	HDAC3	IL-1 β , IL-6, IL-10, IL-12p40	LPS + IFN γ	Genetic (siRNA)	RAW 264.7	(37)
		IL-1 β , IL-8	LPS	Chemical (RGFP966)	GM-CSF differentiated human M ϕ	(38)
		IL-6	LPS	Genetic	LPS differentiated BMM ϕ	(46)
		IL-6, IFN- β	LPS	Genetic (KO mice)	BMM ϕ	(47)
		TNF- α	LPS	Genetic (siRNA/overexpression)	U937	(48)
		IL-6, TNF- α	LPS	Genetic (siRNA)	BV2	(49)
Ila	HDAC4	IL-6, TNF- α	LPS	Genetic (siRNA)	BV2	(49)
Ila	HDAC5	IL-6, IL-10, MCP-1, TNF- α	LPS	Genetic (siRNA/overexpression)	RAW 264.7	(50)
		IL-1 β , IL-6, TNF- α	<i>Mycoplasma pneumoniae</i>	Genetic (siRNA/overexpression)	THP-1	(51)
Iib	HDAC6	IL-10, IL-12p40, IFN- γ	<i>Mtb</i>	Genetic (siRNA/overexpression)	THP-1	(52)
		IL-1 β	LPS + ATP	Genetic (shRNA)	BMM ϕ	(53)
		IL-1 β , IL-6, TNF- α	Unstimulated	Genetic (overexpression)	RAW 264.7	(54)
		IL-6, TNF- α	LPS	Chemical (Tubastatin A)	RAW 264.7, M-CSF differentiated BMM ϕ	(13)
		IL-10	LPS	Genetic (shRNA)	RAW 264.7, PM ϕ	(55)
		IL-10	LPS	Genetic (overexpression)	IL-4 + GM-CSF differentiated BMDC	(56)
Ila	HDAC7	IL-6, TNF- α	LPS	Chemical (Tubastatin A)	THP-1	(57)
		IL-6, IL-12p40, TNF- α	LPS	Genetic (overexpression)	RAW 264.7	(12)
I	HDAC8	IL-6*, IL-1 β , TNF- α *	LPS	Chemical (WK2-16)	THP-1	(58)
	HDAC9	IL-1 β , IL-6, TNF- α	LPS	Genetic (siRNA)	RAW 264.7	(59)
Iib	HDAC10	Unknown				
IV	HDAC11	IL-10, IL-12p40, IFN- γ	<i>Mtb</i>	Genetic (siRNA/overexpression)	THP-1	(52)
		IL-10	LPS	Genetic (shRNA)	RAW 264.7	(55)
		IL-10, IL-12p70	LPS	Genetic (overexpression)	RAW 264.7, THP-1	(56)
		IL-10, IL-12p70	<i>Leishmania donovani</i>	Genetic (overexpression)	IL-4 + GM-CSF differentiated human DC	(60)
		IL-10, IL-12p70	Unstimulated	Genetic (siRNA/overexpression)	RAW 264.7	(61)
		IL-10	LPS	Genetic (siRNA)	THP-1, NOMO-1	(62)
		IL-10, IL-12p70	LPS	Genetic (siRNA)	RAW 264.7	(63)

Positive regulation of cytokines/chemokines is shown in red, negative regulation is indicated in blue. * Findings have been validated in vivo in mice. PM ϕ , peritoneal elicited macrophages; BMM ϕ , bone marrow-derived macrophages; BMDC, bone marrow-derived dendritic cells.



to measure a phenotype in *Mtb*-infected cells (65). Pan-HDAC inhibition by TSA significantly reduced bacterial load in both M ϕ 1 and M ϕ 2 while selective inhibition of class IIa HDACs by TMP195 and TMP269 decreased intracellular *Mtb* outgrowth predominantly in M ϕ 2 (Figure 2B). None of the compounds directly affected bacterial growth in liquid bacterial cultures while a suboptimal dose of the classical *Mtb* antibiotic rifampicin significantly inhibited *Mtb* (Figure 2C), confirming that HDAC inhibitors solely act via host-directed mechanisms and lack direct antimicrobial activity. Collectively, these data identify HDAC enzymes as a novel and important class of proteins in host regulatory networks that control intracellular bacterial survival. Furthermore, targeting HDACs with small molecules to regulate downstream inflammatory pathways could potentially be a novel host-directed therapeutic option for *Mtb* infections.

HDAC Inhibition During Differentiation Polarizes Macrophages Into a More Bactericidal Phenotype

Next, we investigated whether HDAC inhibitors could divert monocytes from the classical M ϕ 1 and M ϕ 2 differentiation pathways to cell subsets exhibiting distinct characteristics

including an increased bactericidal phenotype. Monocytes were exposed to low concentrations of HDAC inhibitors during our standard GM-CSF driven M ϕ 1 or M-CSF driven M ϕ 2 differentiation protocol (Figure 3A). Macrophages differentiated in the presence of HDAC inhibitors were more effective in restricting intracellular bacterial growth in both M ϕ 1 and M ϕ 2 compared to DMSO control treated cells. The pan-HDAC inhibitor TSA was slightly more effective in controlling intracellular *Mtb* infection than the selective class IIa HDAC inhibitors TMP195 and TMP269 (Figure 3B, red dots). Importantly, the observed reduction in *Mtb* outgrowth in macrophages differentiated in the presence of HDAC inhibitors was not due to decreased cell viability (Figure 3C, red dots) or a diminished capacity to phagocytose (Figure 3D), implying a strongly increased intrinsic capacity to control intracellular bacterial survival. Of note, TMP195 consistently increased the phagocytic capacity as well as the percentage of phagocytic cells, especially in M ϕ 1 (Figure 3D and Figure S2), suggesting that the marginal reduction in bacterial load by M ϕ 1 differentiated with TMP195 is considerably underestimating the increased bactericidal capacity induced by TMP195.

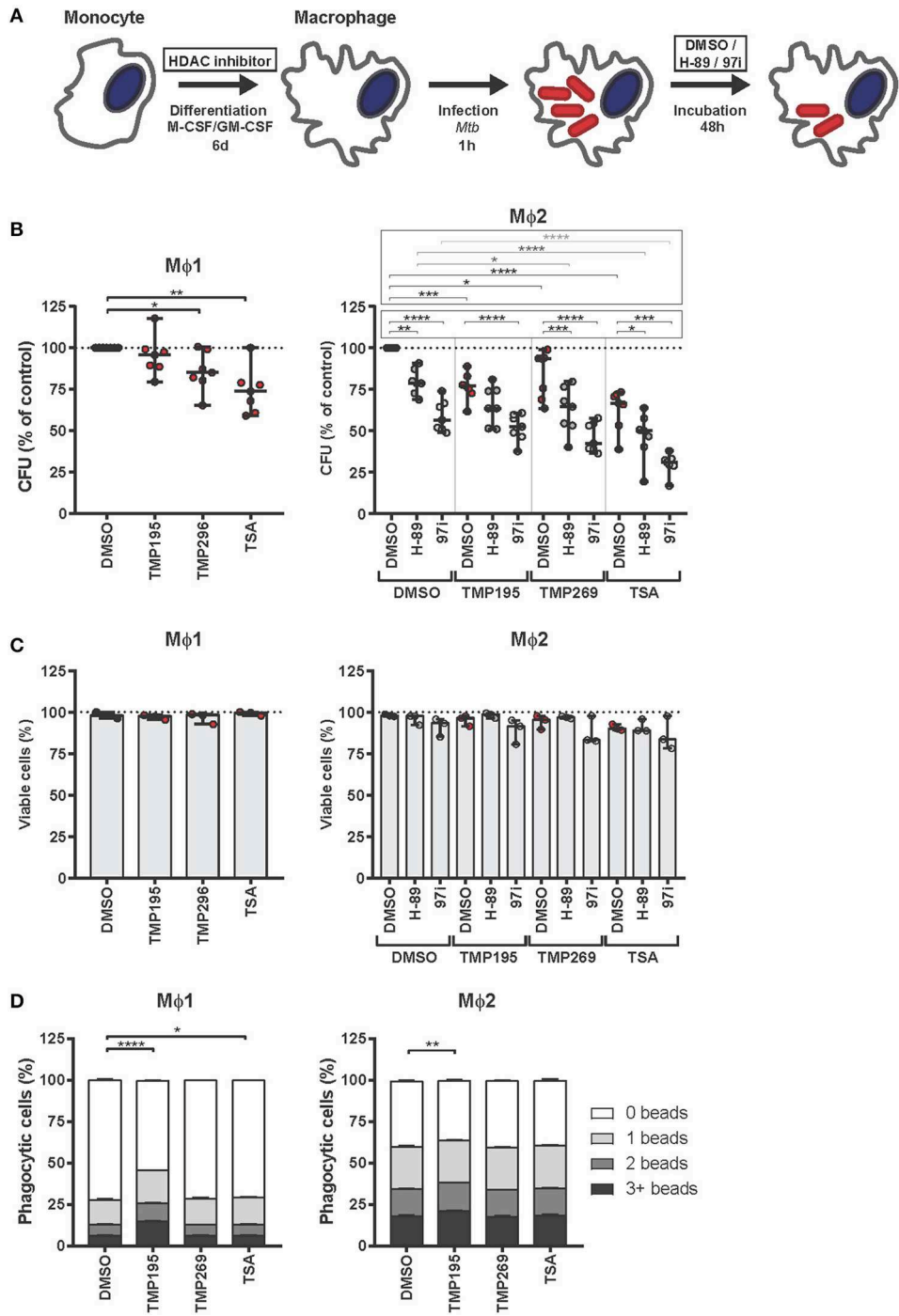
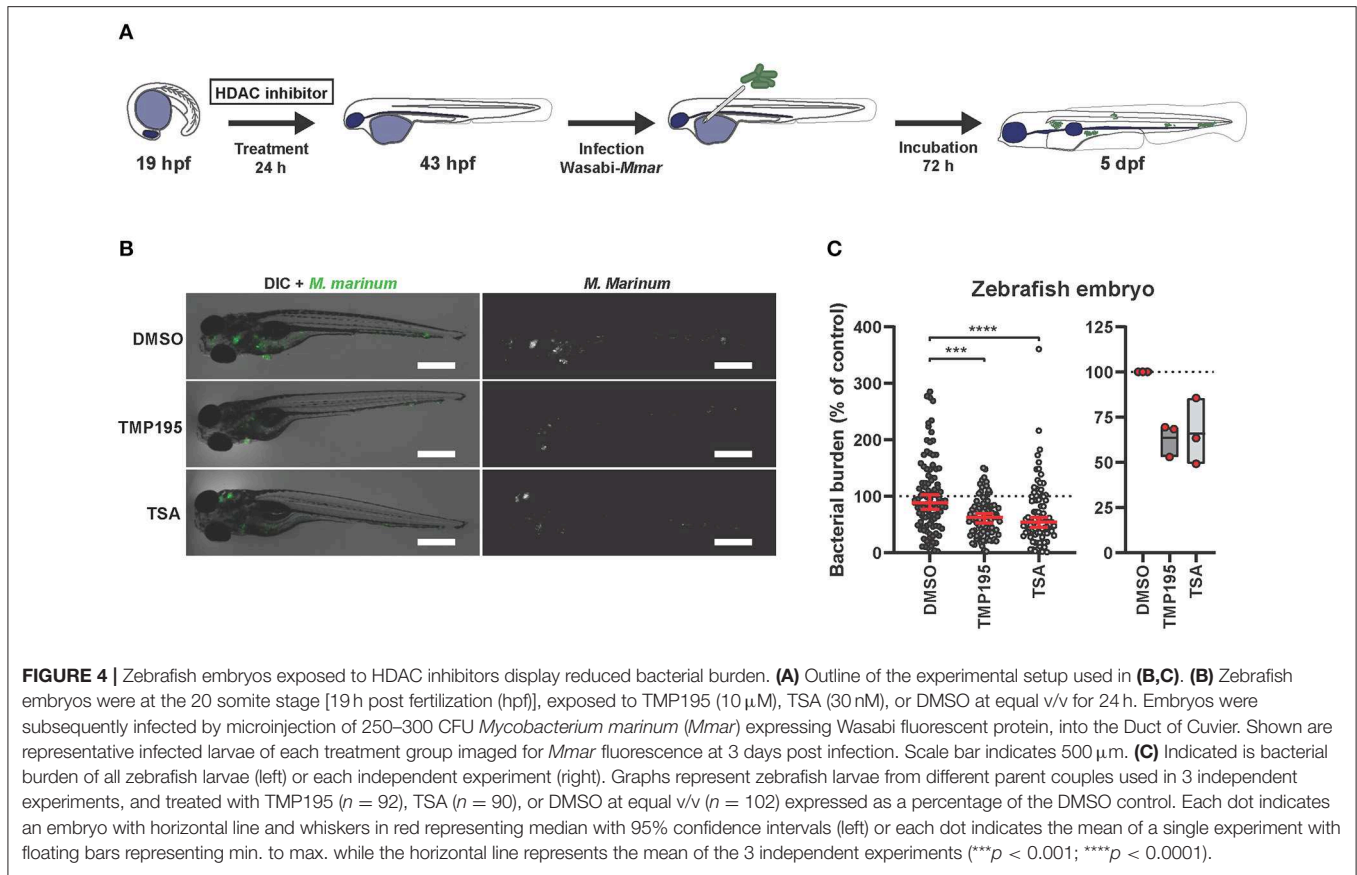


FIGURE 3 | Macrophages exposed during differentiation to low concentrations of HDAC inhibitors are more bactericidal. **(A)** Outline of the experimental setup used in **(B–D)**. **(B)** Monocytes derived from 7 different donors were differentiated toward Mφ1 and Mφ2 while being exposed to TMP195 (300 nM), TMP269 (300 nM), TSA (30 nM), or DMSO at equal v/v for 6 days. Differentiated Mφ1 and Mφ2 were subsequently infected with *Mtb* for 1 h at MOI 10 and incubated for 48 h post-infection until readout. Dots represent the mean of 3 CFU assay replicates of a single donor expressed as a percentage of the DMSO control. Horizontal lines indicate median CFU values of all 7 donors and whiskers represent 95% confidence intervals. Statistically significant differences compared to DMSO were tested using a RM one-way ANOVA (* $p < 0.05$; ** $p < 0.01$; *** $p < 0.001$; **** $p < 0.0001$). **(C)** Cell viability measurement of *Mtb*-infected Mφ1 and Mφ2 (experimental setup as in **B**). Dots represent the mean of 3 cell viability assay replicates of a single donor expressed as a percentage of the DMSO control. Bars indicate median values of all 3 donors and whiskers represent 95% confidence intervals. Statistically significant differences compared to DMSO were tested using a RM one-way ANOVA. **(D)** Phagocytic capacity of Mφ1 and Mφ2 was evaluated by flow-cytometry using fluorescent beads (experimental setup as in **B**). Macrophages were categorized into populations containing either 0, 1, 2, or 3+ beads. Bars depict mean \pm standard deviation of 3 replicates. Data shown is 1 representative donor out of 4. Statistically significant differences compared to DMSO were tested using a one-way ANOVA with Dunnett's multiple test correction (* $p < 0.05$; ** $p < 0.01$; **** $p < 0.0001$).



Since (1) upregulation of HDAC1 expression in *Mtb*-infected macrophages (Figure 1) has been postulated to involve the PKA-CREB-cJun signaling pathway (18) and (2) PKA inhibitor H-89 has previously been shown by us to counteract the manipulation of host signaling processes by *Mtb* (24, 66), we next investigated whether the restriction in bacterial outgrowth in macrophages differentiated in the presence of HDAC inhibitor could be further reduced by treating these macrophages subsequently with PKA inhibitors H-89 or 97i (an H-89 structural analog) following *Mtb*-infection in M ϕ 2 (Figure 3B, gray dots). Because the effect of HDAC inhibitors on *Mtb* bacterial survival was more prominent in M ϕ 2 than M ϕ 1 (Figure 2B), we additionally investigated the putative additive effect of HDAC and PKA host-directed compound combination in M ϕ 2 only. As shown in Figure 3B, a clear additive effect was observed between HDAC and PKA inhibitors in M ϕ 2 with the strongest reduction in bacterial load in 97i-treated TSA-differentiated macrophages (median reduction of 69%), without resulting in significant toxicity (Figure 3C, gray dots).

In summary, these data propose a key role for chromatin remodeling by histone acetylation in orchestrating host defense in TB. Thus, functional inhibition of HDACs may be a promising (host-directed) therapeutic addition to drug-combination regimens already in use for TB.

HDAC Inhibition Reduces Bacterial Burden *in vivo*

To investigate the efficacy of HDAC inhibition *in vivo*, we employed a *Mycobacterium marinum* (*Mmar*) zebrafish embryo infection model. This model has been shown very effective for both fundamental and translational studies in the context of TB research (20–22, 67, 68). Since treatment with HDAC inhibitors during human macrophage differentiation followed by infection showed the highest drug efficacy as described above, we translated the human *in vitro* model to *in vivo* zebrafish embryos by treating them starting at the 20 somite stage, at which the first macrophages appear (69). At 24 h post treatment, embryos were infected with *Mmar* and 3 days after infection, zebrafish embryos were imaged to quantify bacterial burden (Figure 4A). Both TMP195 and TSA pre-treatment reduced bacterial burden *in vivo*, with an average reduction of 37 and 32%, respectively (Figures 4B,C). Importantly, no developmental toxicity was observed. These *in vivo* results strongly support and strengthen our *in vitro* human macrophage results (Figure 3B).

HDAC Activity Regulates Cytokine Production by Macrophages in Response to *Mtb* Infection

Since HDAC activity has been implicated in guiding pro- vs. anti-inflammatory responses, we evaluated whether

exposure to low concentrations HDAC inhibitors during monocyte differentiation altered the phenotype of pro-inflammatory M ϕ 1 and anti-inflammatory M ϕ 2. Expression levels of cell surface markers discriminating between M ϕ 1 and M ϕ 2 (CD14, CD1a, CD163, CD11b) or monitoring the activation status of macrophages (CD80 and CD86) were not affected, except for CD14 whose expression level was upregulated in a proportion of TSA-differentiated M ϕ 1 (**Figure S3A**). Consistent with these findings, no morphological changes were observed in HDAC inhibitor-exposed M ϕ 1 and M ϕ 2 compared to DMSO controls (**Figure S3B**).

Before exploring whether exposure to low concentrations HDAC inhibitors during monocyte differentiation altered the cytokine/chemokine response of pro-inflammatory M ϕ 1 and anti-inflammatory M ϕ 2 upon *Mtb* infection, we first investigated the cytokine/chemokine responses of standardly differentiated M ϕ 1 and M ϕ 2 following infection with *Mtb*. Expression levels of 41 analytes were assessed in the supernatants of *Mtb*-infected M ϕ 1 and M ϕ 2 and compared to uninfected controls 24 h after infection. Both anti-inflammatory cytokines (IL-10, IL-1ra) and pro-inflammatory cytokines (TNF- α , IL-6, GM-CSF, IL-1 β , G-CSF, IL-12p40, and IL-17a) were upregulated in M ϕ 1 and M ϕ 2 but, as expected, the induction of pro-inflammatory cytokines was superior in M ϕ 1 compared to M ϕ 2 whereas the induction of anti-inflammatory cytokine IL-10 was highest in M ϕ 2, confirming and extending our previous findings (**Figure 5A** and **Supplementary Table 1**). To identify those cytokines/chemokines that highly discriminated between the innate responses of M ϕ 1 and M ϕ 2, a multilevel Partial Least Squares-Discriminant Analysis (PLS-DA) was performed. A PLS-DA rotates the PCA components to obtain maximal separation, producing Variable Importance in Projection (VIP) scores for each variable (e.g., analyte), reflecting the importance of each variable to the obtained separation (**Figure S4A**). In parallel, the association of each cytokine/chemokine secretion level with either M ϕ 1 or M ϕ 2 24 h after *Mtb* infection was calculated using Kendall's tau-b correlation test and plotted against the VIP scores (**Figure 5C**). These combined analyses identified MDC, IL-1ra, GM-CSF, TNF- α , and IL-12p40 as having moderate-to-strong correlations with *Mtb*-induced innate responses in M ϕ 1, while for M ϕ 2 MCP-1, IL-10, Eotaxin, and GRO were either uncovered or confirmed.

Next, we investigated the effect of exposure to low dose HDAC inhibitors during monocyte differentiation on the cytokine/chemokine response of M ϕ 1 and M ϕ 2 following *Mtb* infection (**Figure 5B** and **Supplementary Table 1**). Exposure to pan-HDAC inhibitor TSA and class IIa HDAC inhibitors TMP195 and TMP269 potentially dampened the production of both anti- and pro-inflammatory cytokines as well as the majority of chemokines tested in M ϕ 1 in response to *Mtb* infection. In contrast, exposure to HDAC inhibitors during differentiation had limited impact on the innate response of M ϕ 2 with several cytokines/chemokines being slightly lowered in their production while the production of others was only marginally enhanced. To identify cytokines/chemokines most

strongly associated with HDAC inhibition, PLS-DA analyses were performed separately for M ϕ 1 and M ϕ 2 and Kendall's correlation coefficients were calculated for every HDAC inhibitor-induced cytokine/chemokine response (**Figure 5D** and **Figure S4B**). In M ϕ 1, G-CSF, and IFN- γ displayed a clear negative correlation with pan-HDAC and selective class IIa HDAC inhibition, while IL-6, MCP-1 and MIP-1 α showed a negative correlation specifically with class IIa inhibition. In contrast, only weak correlations were observed for M ϕ 2 (except for MIP-1 α , IL-1 β , and IL-8 upon TMP269 exposure), confirming a limited effect of exposure to low concentrations HDAC inhibitors during differentiation toward M ϕ 2 on cytokines/chemokines responses following infection with *Mtb*.

To investigate whether RNA levels correlated with decreased cytokine and chemokine secretion, RNA levels encoding 8 molecules whose secretion was inhibited in response to HDAC inhibition (**Figures 5B,D**), were measured using qPCR in M ϕ 1, since the most profound changes were observed in this macrophage subset (**Figure S4C**). For CCL2 (MCP-1) and CCL4 (MIP-1 β), a clear correlation between transcript and chemokine secretion levels was found, in contrast to CXCL8 (IL-8) and CCL3 (MIP-1 α). For several cytokines, such as IL-6, G-CSF, and IFN- γ , that were secreted in low amounts, we could not detect alterations in RNA levels. Interestingly, TNF transcripts could not be detected despite the fact that secretion of TNF- α levels was found to exceeded 1 μ g/ml which suggests that post transcriptional regulation plays a major role in TNF secretion. Because both G-CSF and IFN- γ negatively correlated with HDAC inhibition in *Mtb*-infected M ϕ 1 and IFN- γ is known to play a major role in TB pathogenesis (70), we further explored the possible role of IFN- γ in M ϕ 1 that were differentiated in the presence of HDAC inhibitors (**Figure S5A**). Addition of IFN- γ to *Mtb*-infected M ϕ 1 decreased the efficacy of HDAC inhibition (**Figure S5B**), without affecting cell viability (**Figure S5C**). Moreover, while HDAC inhibition during differentiation did not affect transcript levels of HDAC1 and HDAC 5 in *Mtb*-infected M ϕ 1 (**Figure S5D**), presence of IFN- γ induced a significant downregulation of HDAC1 expression levels, particularly in M ϕ 1 differentiated in the presence of TSA (**Figure S5E**). Together with its strong upregulation upon infection (**Figure 1** and **Figure S1**), this supports an important role for HDAC1 during infection with *Mtb*.

Collectively, HDAC inhibition during macrophage differentiation profoundly downregulated inflammatory cytokine production induced by *Mtb* infection, particularly in M ϕ 1. For several chemokines, this clearly correlated with lowered transcript levels while this correlation was absent for others, suggesting post-transcriptional modification also plays a role. Since *Mtb* can exploit host cytokine signaling networks for its survival and a delicate balance between pro- and anti-inflammatory cytokines is required to restrict *Mtb* proliferation (71), these data suggest that HDACs may affect the outcome of *Mtb* infection by altering infection-induced orchestrated cytokine/chemokine responses by innate immune cells.

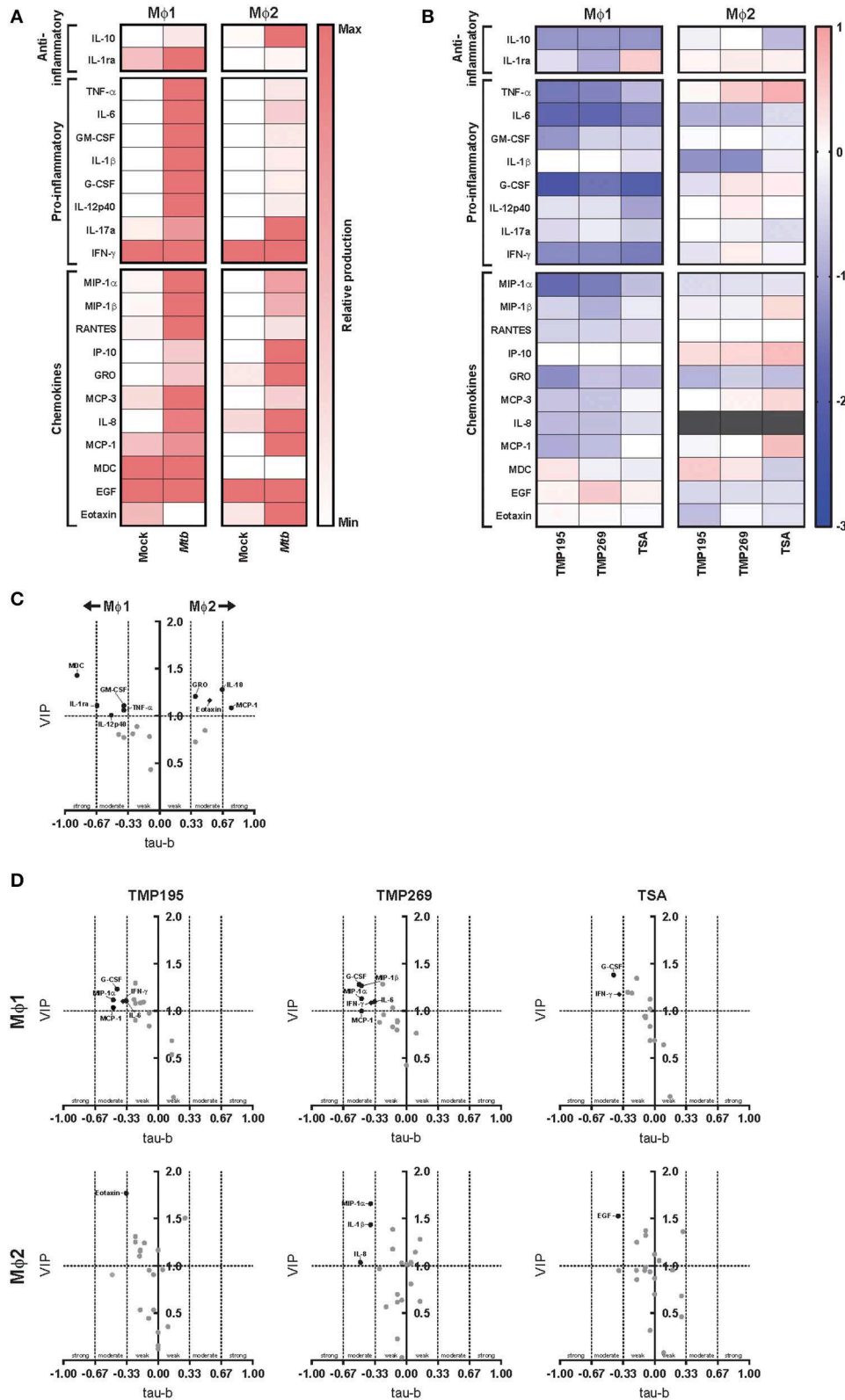


FIGURE 5 | Exposure to low concentrations HDAC inhibitors during monocyte differentiation alters the cytokine/chemokine response of Mφ1 and Mφ2 upon *Mtb* infection. **(A)** Heat map displaying median cytokine/chemokine expression levels (of 4 different donors) in supernatants of standardly differentiated Mφ1 and Mφ2 24 h (Continued)

FIGURE 5 | following *Mtb* or mock infection. Each row represents the relative expression of the indicated cytokine/chemokine using a white to red color scale. Of the 41 analytes measured, only cytokines/chemokines that changed in at least 3 out of 4 donors and exhibited a minimal median \log_2 fold change (FC) of 0.5 in a single comparison are shown. **(B)** Heat map displaying median \log_2 FC of cytokine/chemokine levels in supernatants of M ϕ 1 and M ϕ 2 of 4 different donors. In this experimental setup monocytes were exposed to TMP195 (300 nM), TMP269 (300 nM), TSA (30 nM), or DMSO at equal v/v during differentiation toward M ϕ 1 and M ϕ 2. Gray color depicts cytokine/chemokine levels that were detected above the linear range of the assay. **(C)** Experimental setup as in **(A)**. Variable Importance in Projection (VIP) scores of the first x-variate were extracted from each PLS-DA analysis and cytokine values ≥ 1 were considered relevant. In parallel, Kendall's tau-b correlation coefficients were calculated for each cytokine. Coefficients between 0–0.33, 0.33–0.67, and 0.67–1 were considered to have a weak, moderate and strong correlation, respectively. Every dot represents a cytokine/chemokine. Cytokines/chemokines with a VIP score > 1 and demonstrating at least a moderate correlation are annotated in black. Annotated cytokines that were produced below or equal to a median concentration of 40 pg/ml are depicted by a diamond. **(D)** Experimental setup as in **(B)**. VIP scores and Kendall's tau-b correlation coefficients calculations as in **(C)**.

DISCUSSION

Here, we report that histone deacetylase (HDAC) transcriptomic levels are strongly affected by *Mtb*-infection in primary human macrophages. Secondly, we report that broad chemical HDAC inhibition can enhance the antimicrobial response of both M ϕ 1 and M ϕ 2, while selective inhibition of class IIa HDACs prominently decreased bacterial outgrowth in M ϕ 2. Thirdly, chemical inhibition of HDAC activity during differentiation polarized macrophages into a more bactericidal phenotype with a concomitant decrease in the secretion levels of inflammatory cytokines. Fourth, *in vivo* chemical inhibition of HDAC activity in *Mycobacterium marinum* infected zebrafish embryos, a well-characterized animal model for tuberculosis, significantly reduced mycobacterial burden *in vivo*, validating our *in vitro* findings in primary human macrophages. Collectively, these data identify HDACs as druggable host targets for HDT against intracellular *Mtb*.

Previous studies have suggested that *Mtb* can modulate host defense by epigenetic modifications to facilitate survival within the host cell (16, 18, 19). In this study, we observed that following *Mtb* infection, transcriptional levels of several HDACs representing different classes were differentially regulated in M ϕ 1 but primarily in M ϕ 2. Our findings, which are in agreement with (in this paper) independently analyzed results from Blischak et al. (64), identify HDAC enzymes as potential targets for immune modulation in infectious diseases. This idea is supported by similar expression levels of several HDACs when comparing M ϕ 2 infected with a virulent *Mtb* strain to uninfected controls. Since macrophage differentiation states are known to be dynamic and flexible, macrophages represent highly interesting therapeutic targets, both in differentiated (e.g., M ϕ 1 and M ϕ 2) and in less differentiated stages. Interestingly, treatment with the pan-HDAC inhibitor TSA decreased bacterial survival in both *Mtb*-infected M ϕ 1 and M ϕ 2 while selective class IIa HDAC inhibitors TMP195 and TMP269 decreased *Mtb* survival predominantly in M ϕ 2. This is one of the first studies comparatively analyzing HDT in M ϕ 1 and M ϕ 2 in a human infection model, indicating that downregulation of HDAC activity in the context of *Mtb* infection can be beneficial to host control of infection. The attenuated efficacy of class IIa HDAC inhibitors on *Mtb* survival in M ϕ 1 might be explained by the lower basal expression levels of HDAC5 and HDAC7 in M ϕ 1 compared to M ϕ 2 (**Figure S1A**), which could suggest that the therapeutic window of these inhibitors is significantly larger in M ϕ 2.

A recent cohort study in Uganda compared whole genome transcriptional profiles of *Mtb*-infected monocytes derived from peripheral blood of household contacts of TB patients who were resistant to *Mtb* infection (resisters) with individuals who were susceptible to *Mtb* infection [latent TB infection (LTBI)] (72, 73). Consistent with our observation that HDAC function is important for the innate immune response to *Mtb* infection, they showed that pathways controlled by HDACs were markedly differentially activated between the two study groups. The clinical potential of HDAC inhibition in the context of TB has already been proven by studies showing reduced bacterial burden in an *in vivo* mouse model using Tubustatin A, a HDAC6 inhibitor (74). Here, we significantly expand upon this work by demonstrating the potential of both a selective class IIa inhibitor and a pan-HDAC inhibitor, TMP195 and TSA, respectively, for treating mycobacterial infection in an *in vivo* model. Zebrafish embryos pre-treated with TMP195 or TSA, at concentrations not inducing developmental toxicity, showed a clear reduction in mycobacterial infection burden. A useful characteristic of the *Mmar* zebrafish embryo infection model is the lack of functional adaptive immune cells, thus allowing the assessment of innate immunity only (75). Despite the absence of T-cells, macrophage aggregates with granuloma-like features nevertheless are formed, a critical feature of TB (76). Therefore, our results support the effectivity of HDAC inhibitors during early stages of TB granuloma formation. Future work should be directed toward dissecting the effect of these HDT compounds in the presence of adaptive immunity and mature TB granulomas. Collectively, the independent data sets reported in our study and by others (74) strongly suggest that HDACs are an important factor in the innate immune response to *Mtb* infection, and that their inhibition can enhance antimicrobial activity of infected macrophages.

Interestingly, we found that targeting HDACs in monocytes during differentiation to either M ϕ 1 or M ϕ 2 strongly improved the ability of the host to control subsequent *Mtb* infection. In agreement with our finding, Guerriero et al., demonstrated in an *in vivo* mouse cancer model that treatment with class IIa HDAC inhibitor TMP195 increased the anti-tumor potential of macrophages by pharmacologic modulation of the macrophage phenotype (26). Importantly, in our *in vitro* *Mtb*-macrophage infection model, a combinatorial regimen of HDAC and PKA/PKB inhibitors resulted in a clearly additive effect in decreasing intracellular bacterial survival in M ϕ 2 (**Figure 3B**). The PKA/PKB inhibitor H-89 has been shown

to regulate a kinase network around AKT1/PKB-AS160-RAB14 that controls the intracellular survival of *Mtb* and *Salmonella* by manipulating phagosome maturation and actin remodeling (24, 66). Furthermore, PKA is known to be involved in numerous other signaling pathways associated with *Mtb* survival (77, 78). Moreover, PKA inhibition might also have impaired class IIa HDAC function by interfering with nucleocytoplasmic trafficking since PKA activation promotes nuclear import of HDAC4 by phosphorylation and inhibits class IIa HDAC nuclear export via the LKB1-SIK2/3 axis (79, 80). Demonstration of synergistic effects of TSA and PKA/PKB inhibitors is in line with results by Zhu et al. (81), who demonstrated upregulation of the PI3K-AKT1 signaling pathway in *Mtb*-infected THP-1 cells treated with TSA. Of note, Zhu et al. (81) reported TSA to promote *Mtb* survival but this discrepancy is likely explained by the use of the THP-1 cell line which requires stimulation with phorbol 12-myristate 13-acetate (PMA) as opposed to primary macrophages, as well as the higher concentration (625 nM) of TSA they used, which was highly toxic in our model. Our work is one of the first demonstrations of synergism (82) between different HDT compounds in the control of bacterial pathogens and provides an important avenue for further studies in this area. We speculate that the simultaneous targeting of mechanistically different host pathways underlies this synergism.

The kinetics and quantities of cytokines released by the host during infection is an important aspect influencing the outcome of immune responses against *Mtb* (71, 83). Surprisingly, while HDAC inhibition during monocyte differentiation restricted intracellular bacterial outgrowth more effectively in *Mtb*-infected M ϕ 2 than M ϕ 1 (Figure 3B), the cytokine/chemokine secretion profile was only moderately altered in M ϕ 2 (Figure 4B). In contrast, M ϕ 1 exposed during differentiation to HDAC inhibitors clearly displayed a less pro-inflammatory phenotype, raising the question which HDAC inhibitor-induced cytokine/chemokine profile is optimal for host resistance against *Mtb*. In line with this, the addition of IFN- γ , a protein known to be vital in TB pathogenesis (70), impaired the effect of HDAC inhibition on bacterial survival in M ϕ 1. Lastly, TSA-enhanced M ϕ 2 polarization was demonstrated to be dependent on TSA-induced autophagy (84), a process vital for the clearance of *Mtb* (85). Future work will need to explore the role of autophagy in *Mtb*-infected macrophages treated with HDAC inhibitors.

Interestingly, it has been shown that both silencing and chemical inhibition of class IIa HDACs induces the expression of transcription factor Nur77, an orphan nuclear receptor and immediate-early gene that regulates cellular proliferation, apoptosis, inflammation, and glucose metabolism (86). Nur77 has been demonstrated to promote anti-inflammatory function by rewiring the tricarboxylic acid (TCA) cycle in pro-inflammatory macrophages (87). Moreover, Nur77-deficiency was found to drive macrophage polarization toward a pro-inflammatory phenotype, characterized by increased IL-6, IL-12, and IFN- γ production, among others (88, 89). Despite the fact that specific effects of different HDACs on inflammatory profiles are just beginning to be elucidated (Table 1), we

hypothesize that modulation of cytokine/chemokine secretion is a likely mechanism by which *Mtb* can evade from host defense and propose that this may be therapeutically counteracted by inhibiting HDAC-mediated transcriptional regulation (71).

Although, HDAC inhibitors are well-known for their regulation of transcriptional activity by histone deacetylation, their function may not be limited to modulating epigenetic changes. For example, it has been shown by Gregoire et al. that the function of transcription factor MEF2 can be inhibited through class IIa HDAC-mediated sumoylation (90, 91). Regulation of these alternative functions may also have contributed to an enhanced bactericidal capacity of HDAC inhibitor-treated macrophages. Therefore, a more complete understanding of the complex function of HDAC enzymes and their effect on cellular and immuno-modulatory processes will be necessary to understand the full therapeutic potential of their inhibitors.

In summary, our findings demonstrate that HDAC inhibitors offer the possibility to augment antimicrobial responses against *Mtb* infection. Moreover, they can act in synergy with other host-directed strategies and may well-synergize also with current antibiotics to improve TB treatment efficacy and to shortening TB therapies, a major goal in TB research. Although exploitation of HDACs as druggable targets for HDT against intracellular *Mtb* requires further work, our data clearly suggest that pharmacological targeting of host epigenetic regulation could be a promising strategy to improve the innate immune response against *Mtb*.

DATA AVAILABILITY STATEMENT

All datasets generated for this study are included in the article/**Supplementary Material**.

AUTHOR CONTRIBUTIONS

JM, BK, SV, MTH, and KW designed and performed the experiments and processed the experimental data. JM, BK, MTH, FV, TM, HS, AM, TO, and MCH contributed to the interpretation of the results. JM, MTH, TO, and MCH wrote the manuscript and designed the figures with input from FV. MCH supervised the project. All authors approved the final version of the manuscript.

FUNDING

This project was funded by grants from the Netherlands Organization for Health Research and Development (ZonMw-TOP grant 91214038), NWO Domain Applied and Engineering Sciences (NWO-TTW grant 13259), the Brazilian Federal Agency for Support and Evaluation of Graduate Education (CAPES), and the EU-ToxRisk project (An Integrated European Flagship Program Driving Mechanism-Based Toxicity Testing and Risk Assessment for the twenty first century) funded by the European Commission under the Horizon 2020 program (Grant Agreement No. 681002). The funders had no role in study design,

data collection and analysis, decision to publish, or preparation of the manuscript.

ACKNOWLEDGMENTS

We gratefully acknowledge Dr. J. Bestebroer (VUMC, Amsterdam, The Netherlands) for mycobacterial reporter constructs and Prof. Dr. H. S. Overkleeft (Leiden Academic

Center for Drug Research, Leiden University, Leiden, The Netherlands) for synthesizing H-89 analog 97i.

SUPPLEMENTARY MATERIAL

The Supplementary Material for this article can be found online at: <https://www.frontiersin.org/articles/10.3389/fimmu.2020.00036/full#supplementary-material>

REFERENCES

- WHO. *Global Tuberculosis Report*. Geneva: World Health Organization (2019).
- Becker D, Selbach M, Rollenhagen C, Ballmaier M, Meyer TF, Mann M, et al. Robust *Salmonella* metabolism limits possibilities for new antimicrobials. *Nature*. (2006) 440:303. doi: 10.1038/nature04616
- Srivastava S, Ernst JD, Desvignes L. Beyond macrophages: the diversity of mononuclear cells in tuberculosis. *Immunol Rev*. (2014) 262:179–92. doi: 10.1111/immr.12217
- Upadhyay S, Mittal E, Philips JA. Tuberculosis and the art of macrophage manipulation. *Pathog Dis*. (2018) 76:1–12. doi: 10.1093/femspd/fty037
- Benoit M, Desnues B, Mege J-L. Macrophage polarization in bacterial infections. *J Immunol*. (2008) 181:3733–9. doi: 10.4049/jimmunol.181.6.3733
- Khosla S, Sharma G, Yaseen I. Learning epigenetic regulation from mycobacteria. *Microb Cell*. (2016) 3:92. doi: 10.15698/mic2016.02.480
- Patel U, Rajasingh S, Samanta S, Cao T, Dawn B, Rajasingh J. Macrophage polarization in response to epigenetic modifiers during infection and inflammation. *Drug Discov Today*. (2017) 22:186–93. doi: 10.1016/j.drudis.2016.08.006
- Verdone L, Caserta M, Di Mauro E. Role of histone acetylation in the control of gene expression. *Biochem Cell Biol*. (2005) 83:344–53. doi: 10.1139/o05-041
- Seto E, Yoshida M. Erasers of histone acetylation: the histone deacetylase enzymes. *Cold Spring Harb Perspect Biol*. (2014) 6:a018713. doi: 10.1101/cshperspect.a018713
- Mulligan SE, Gaddis CA, Alenghat T, Nair MG, Giacomin PR, Everett LJ, et al. Histone deacetylase 3 is an epigenomic brake in macrophage alternative activation. *Genes Dev*. (2011) 25:2480–8. doi: 10.1101/gad.175950.111
- Aung HT, Schroder K, Himes SR, Brion K, van Zuylen W, Trieu A, et al. LPS regulates proinflammatory gene expression in macrophages by altering histone deacetylase expression. *FASEB J*. (2006) 20:1315–27. doi: 10.1096/fj.05-5360.com
- Shakespear MR, Hohenhaus DM, Kelly GM, Kamal NA, Gupta P, Labzin LI, et al. Histone deacetylase 7 promotes toll-like receptor 4-dependent proinflammatory gene expression in macrophages. *J Biol Chem*. (2013) 288:25362–74. doi: 10.1074/jbc.M113.496281
- Yan B, Xie S, Liu Z, Ran J, Li Y, Wang J, et al. HDAC6 deacetylase activity is critical for lipopolysaccharide-induced activation of macrophages. *PLoS One*. (2014) 9:e110718. doi: 10.1371/journal.pone.0110718
- Marino S, Cilfone NA, Mattila JT, Linderman JJ, Flynn JL, Kirschner DE. Macrophage polarization drives granuloma outcome during *Mycobacterium tuberculosis* infection. *Infect Immun*. (2015) 83:324–38. doi: 10.1128/IAI.02494-14
- Huang L, Nazarova EV, Tan S, Liu Y, Russell DG. Growth of *Mycobacterium tuberculosis* in vivo segregates with host macrophage metabolism and ontogeny. *J Exp Med*. (2018) 215:1135–52. doi: 10.1084/jem.20172020
- Wang Y, Curry HM, Zwilling BS, Lafuse WP. Mycobacteria inhibition of IFN- γ induced HLA-DR gene expression by up-regulating histone deacetylation at the promoter region in human THP-1 monocytic cells. *J Immunol*. (2005) 174:5687–94. doi: 10.4049/jimmunol.174.9.5687
- Schmeck B, Lorenz J, N'Guessan PD, Opitz B, van Laak V, Zahltan J, et al. Histone acetylation and flagellin are essential for *Legionella pneumophila*-induced cytokine expression. *J Immunol*. (2008) 181:940–7. doi: 10.4049/jimmunol.181.2.940
- Chandran A, Antony C, Jose L, Mundayoor S, Natarajan K, Kumar RA. *Mycobacterium tuberculosis* infection induces HDAC1-mediated suppression of IL-12B gene expression in macrophages. *Front Cell Infect Microbiol*. (2015) 5:90. doi: 10.3389/fcimb.2015.00090
- Moores RC, Brilha S, Schutgens F, Elkington PT, Friedland JS. Epigenetic regulation of matrix metalloproteinase-1 and -3 expression in *Mycobacterium tuberculosis* infection. *Front Immunol*. (2017) 8:602. doi: 10.3389/fimmu.2017.00602
- Ramakrishnan L. The zebrafish guide to tuberculosis immunity and treatment. *Cold Spring Harb Symp Quant Biol*. (2013) 78:179–92. doi: 10.1101/sqb.2013.78.023283
- Cronan MR, Tobin DM. Fit for consumption: zebrafish as a model for tuberculosis. *Dis Models Mech*. (2014) 7:777–84. doi: 10.1242/dmm.016089
- Meijer AH. Protection and pathology in TB: learning from the zebrafish model. *Semin Immunopathol*. (2016) 38:261–73. doi: 10.1007/s00281-015-0522-4
- Verreck FA, de Boer T, Langenberg DM, van der Zanden L, Ottenhoff TH. Phenotypic and functional profiling of human proinflammatory type-1 and anti-inflammatory type-2 macrophages in response to microbial antigens and IFN- γ - and CD40L-mediated costimulation. *J Leukoc Biol*. (2006) 79:285–93. doi: 10.1189/jlb.0105015
- Korbee CJ, Heemskerk MT, Kocov D, van Strijen E, Rabiee O, Franken K, et al. Combined chemical genetics and data-driven bioinformatics approach identifies receptor tyrosine kinase inhibitors as host-directed antimicrobials. *Nat Commun*. (2018) 9:358. doi: 10.1038/s41467-017-02777-6
- Lobera M, Madauss KP, Pohlhaus DT, Wright QG, Trocha M, Schmidt DR, et al. Selective class IIa histone deacetylase inhibition via a nonchelating zinc-binding group. *Nat Chem Biol*. (2013) 9:nchembio.1223. doi: 10.1038/nchembio.1223
- Guerriero JL, Sotayo A, Ponichtera HE, Castrillon JA, Pourzia AL, Schad S, et al. Class IIa HDAC inhibition reduces breast tumours and metastases through anti-tumour macrophages. *Nature*. (2017) 543:428. doi: 10.1038/nature21409
- Roger T, Lugin J, Le Roy D, Goy G, Mombelli M, Koessler T, et al. Histone deacetylase inhibitors impair innate immune responses to Toll-like receptor agonists and to infection. *Blood*. (2011) 117:1205–17. doi: 10.1182/blood-2010-05-284711
- Takaki K, Davis JM, Winglee K, Ramakrishnan L. Evaluation of the pathogenesis and treatment of *Mycobacterium marinum* infection in zebrafish. *Nat Protoc*. (2013) 8:1114–24. doi: 10.1038/nprot.2013.068
- Benard EL, van der Sar AM, Ellett F, Lieschke GJ, Spaink HP, Meijer AH. Infection of zebrafish embryos with intracellular bacterial pathogens. *J Vis Exp*. (2012) 61:3781. doi: 10.3791/3781
- Stoop EJM, Schipper T, Huber SKR, Nezhinsky AE, Verbeek FJ, Gurcha SS, et al. Zebrafish embryo screen for mycobacterial genes involved in the initiation of granuloma formation reveals a newly identified ESX-1 component. *Dis Models Mech*. (2011) 4:526–36. doi: 10.1242/dmm.006676
- Westergren G, Krasse B. Evaluation of a micromethod for determination of *Streptococcus mutans* and *Lactobacillus* infection. *J Clin Microbiol*. (1978) 7:82–3.
- Livak KJ, Schmittgen TD. Analysis of relative gene expression data using real-time quantitative PCR and the 2⁻ $\Delta\Delta$ CT method. *Methods*. (2001) 25:402–8. doi: 10.1006/meth.2001.1262

33. Westerhuis JA, van Velzen EJ, Hoefsloot HC, Smilde AK. Multivariate paired data analysis: multilevel PLSDA versus OPLSDA. *Metabolomics*. (2010) 6:119–28. doi: 10.1007/s11306-009-0185-z
34. Rohart F, Gautier B, Singh A, Le Cao K-A. mixOmics: an R package for 'omics feature selection and multiple data integration. *PLoS Comp Biol*. (2017) 13:e1005752. doi: 10.1371/journal.pcbi.1005752
35. Hipel KW, McLeod AI. *Time Series Modelling of Water Resources and Environmental Systems. Developments in Water Science*. (Geneva) (1994) 80:60.
36. Schindelin J, Arganda-Carreras I, Frise E, Kaynig V, Longair M, Pietzsch T, et al. Fiji: an open-source platform for biological-image analysis. *Nat Methods*. (2012) 9:676–82. doi: 10.1038/nmeth.2019
37. Leus NG, van der Wouden PE, van den Bosch T, Hooghiemstra WT, Ourailidou ME, Kistemaker LE, et al. HDAC 3-selective inhibitor RGFP966 demonstrates anti-inflammatory properties in RAW 264.7 macrophages and mouse precision-cut lung slices by attenuating NF-kappaB p65 transcriptional activity. *Biochem Pharmacol*. (2016) 108:58–74. doi: 10.1016/j.bcp.2016.03.010
38. Winkler AR, Nocka KN, Williams CM. Smoke exposure of human macrophages reduces HDAC3 activity, resulting in enhanced inflammatory cytokine production. *Pulm Pharmacol Ther*. (2012) 25:286–92. doi: 10.1016/j.pupt.2012.05.003
39. Leus NG, van den Bosch T, van der Wouden PE, Krist K, Ourailidou ME, Eleftheriadis N, et al. HDAC1-3 inhibitor MS-275 enhances IL10 expression in RAW264.7 macrophages and reduces cigarette smoke-induced airway inflammation in mice. *Sci Rep*. (2017) 7:45047. doi: 10.1038/srep45047
40. Zhang ZY, Schluessener HJ. HDAC inhibitor MS-275 attenuates the inflammatory reaction in rat experimental autoimmune prostatitis. *Prostate*. (2012) 72:90–9. doi: 10.1002/pros.21410
41. Nencioni A, Beck J, Werth D, Grünebach F, Patrone F, Ballestrero A, et al. Histone deacetylase inhibitors affect dendritic cell differentiation and immunogenicity. *Clin Cancer Res*. (2007) 13:3933–41. doi: 10.1158/1078-0432.CCR-06-2903
42. Kaneko J, Okinaga T, Ariyoshi W, Hikiji H, Fujii S, Iwanaga K, et al. Ky-2, a hybrid compound histone deacetylase inhibitor, regulated inflammatory response in LPS-driven human macrophages. *Cell Biol Int*. (2018) 42:1622–31. doi: 10.1002/cbin.11058
43. Fang WF, Chen YM, Lin CY, Huang HL, Yeh H, Chang YT, et al. Histone deacetylase 2 (HDAC2) attenuates lipopolysaccharide (LPS)-induced inflammation by regulating PAI-1 expression. *J Inflamm*. (2018) 15:3. doi: 10.1186/s12950-018-0179-6
44. Wu C, Li A, Hu J, Kang J. Histone deacetylase 2 is essential for LPS-induced inflammatory responses in macrophages. *Immunol Cell Biol*. (2018) 97:72–84. doi: 10.1111/imcb.12203
45. Zhang Q, Zhao K, Shen Q, Han Y, Gu Y, Li X, et al. Tet2 is required to resolve inflammation by recruiting Hdac2 to specifically repress IL-6. *Nature*. (2015) 525:389–93. doi: 10.1038/nature15252
46. Sanchez S, Lemmens S, Baeten P, Sommer D, Dooley D, Hendrix S, et al. HDAC3 inhibition promotes alternative activation of macrophages but does not affect functional recovery after spinal cord injury. *Exp Neurol*. (2018) 27:437–52. doi: 10.5607/en.2018.27.5.437
47. Chen X, Barozzi I, Termanini A, Prosperini E, Recchiuti A, Dalli J, et al. Requirement for the histone deacetylase Hdac3 for the inflammatory gene expression program in macrophages. *Proc Natl Acad Sci USA*. (2012) 109:E2865–2874. doi: 10.1073/pnas.1121131109
48. Mahlknecht U, Will J, Varin A, Hoelzer D, Herbein G. Histone deacetylase 3, a class I histone deacetylase, suppresses MAPK11-mediated activating transcription factor-2 activation and represses TNF gene expression. *J Immunol*. (2004) 173:3979–90. doi: 10.4049/jimmunol.173.6.3979
49. Wang B, Liu T-y, Lai C-H, Rao Y-h, Choi M-C, Chi J-T, et al. Glycolysis-dependent histone deacetylase 4 degradation regulates inflammatory cytokine production. *Mol Biol Cell*. (2014) 25:3300–7. doi: 10.1091/mbc.e13-12-0757
50. Poralla L, Stroth T, Erben U, Sittig M, Liebig S, Siegmund B, et al. Histone deacetylase 5 regulates the inflammatory response of macrophages. *J Cell Mol Med*. (2015) 19:2162–71. doi: 10.1111/jcmm.12595
51. Zhao Y, Ma G, Yang X. HDAC5 promotes *Mycoplasma pneumoniae*-induced inflammation in macrophages through NF-kappaB activation. *Life Sci*. (2019) 221:13–9. doi: 10.1016/j.lfs.2019.02.004
52. Wang X, Wu Y, Jiao J, Huang Q. *Mycobacterium tuberculosis* infection induces IL-10 gene expression by disturbing histone deacetylase 6 and histone deacetylase 11 equilibrium in macrophages. *Tuberculosis*. (2018) 108:118–23. doi: 10.1016/j.tube.2017.11.008
53. Hwang I, Lee E, Jeon SA, Yu JW. Histone deacetylase 6 negatively regulates NLRP3 inflammasome activation. *Biochem Biophys Res Commun*. (2015) 467:973–8. doi: 10.1016/j.bbrc.2015.10.033
54. Youn GS, Lee KW, Choi SY, Park J. Overexpression of HDAC6 induces pro-inflammatory responses by regulating ROS-MAPK-NF-kappaB/AP-1 signaling pathways in macrophages. *Free Radic Biol Med*. (2016) 97:14–23. doi: 10.1016/j.freeradbiomed.2016.05.014
55. Cheng F, Lienlaf M, Perez-Villaruel P, Wang HW, Lee C, Woan K, et al. Divergent roles of histone deacetylase 6 (HDAC6) and histone deacetylase 11 (HDAC11) on the transcriptional regulation of IL10 in antigen presenting cells. *Mol Immunol*. (2014) 60:44–53. doi: 10.1016/j.molimm.2014.02.019
56. Villagra A, Cheng F, Wang HW, Suarez I, Glozak M, Maurin M, et al. The histone deacetylase HDAC11 regulates the expression of interleukin 10 and immune tolerance. *Nat Immunol*. (2009) 10:92–100. doi: 10.1038/ni.1673
57. Vishwakarma S, Iyer LR, Muley M, Singh PK, Shastri A, Saxena A, et al. Tubastatin, a selective histone deacetylase 6 inhibitor shows anti-inflammatory and anti-rheumatic effects. *Int Immunopharmacol*. (2013) 16:72–8. doi: 10.1016/j.intimp.2013.03.016
58. Jan JS, Chou YC, Cheng YW, Chen CK, Huang WJ, Hsiao G. The novel HDAC8 inhibitor WK2-16 attenuates lipopolysaccharide-activated matrix metalloproteinase-9 expression in human monocytic cells and improves hypercytokinemia *in vivo*. *Int J Mol Sci*. (2017) 18:E1394. doi: 10.3390/ijms18071394
59. Pham TX, Bae M, Lee Y, Park YK, Lee JY. Transcriptional and posttranscriptional repression of histone deacetylases by docosahexaenoic acid in macrophages. *J Nutr Biochem*. (2018) 57:162–9. doi: 10.1016/j.jnutbio.2018.03.002
60. Mukherjee S, Mukherjee B, Mukhopadhyay R, Naskar K, Sundar S, Dujardin JC, et al. Imipramine exploits histone deacetylase 11 to increase the IL-12/IL-10 ratio in macrophages infected with antimony-resistant *Leishmania donovani* and clears organ parasites in experimental infection. *J Immunol*. (2014) 193:4083–94. doi: 10.4049/jimmunol.1400710
61. Shinohara H, Kuranaga Y, Kumazaki M, Sugito N, Yoshikawa Y, Takai T, et al. Regulated polarization of tumor-associated macrophages by miR-145 via colorectal cancer-derived extracellular vesicles. *J Immunol*. (2017) 199:1505–15. doi: 10.4049/jimmunol.1700167
62. Bala S, Csak T, Kodys K, Catalano D, Ambade A, Furi I, et al. Alcohol-induced miR-155 and HDAC11 inhibit negative regulators of the TLR4 pathway and lead to increased LPS responsiveness of Kupffer cells in alcoholic liver disease. *J Leukoc Biol*. (2017) 102:487–98. doi: 10.1189/jlb.3A0716-310R
63. Lin L, Hou J, Ma F, Wang P, Liu X, Li N, et al. Type I IFN inhibits innate IL-10 production in macrophages through histone deacetylase 11 by downregulating microRNA-145. *J Immunol*. (2013) 191:3896–904. doi: 10.4049/jimmunol.1203450
64. Blischak JD, Tailleur L, Mitrano A, Barreiro LB, Gilad Y. Mycobacterial infection induces a specific human innate immune response. *Sci Rep*. (2015) 5:16882. doi: 10.1038/srep16882
65. Roy S, Schmeier S, Kaczkowski B, Arner E, Alam T, Ozturk M, et al. Transcriptional landscape of *Mycobacterium tuberculosis* infection in macrophages. *Sci Rep*. (2018) 8:6758. doi: 10.1038/s41598-018-24509-6
66. Kuijl C, Savage ND, Marsman M, Tuin AW, Janssen L, Egan DA, et al. Intracellular bacterial growth is controlled by a kinase network around PKB/AKT1. *Nature*. (2007) 450:725. doi: 10.1038/nature06345
67. Tobin DM, Vary JC, Ray JP, Walsh GS, Dunstan SJ, Bang ND, et al. The Itah4 locus modulates susceptibility to mycobacterial infection in zebrafish and humans. *Cell*. (2010) 140:717–30. doi: 10.1016/j.cell.2010.02.013
68. van der Vaart M, Korbee CJ, Lamers GE, Tengeler AC, Hosseini R, Haks MC, et al. The DNA damage-regulated autophagy modulator DRAM1 links mycobacterial recognition via TLR-MYD88 to autophagic defense [corrected]. *Cell Host Microbe*. (2014) 15:753–67. doi: 10.1016/j.chom.2014.05.005
69. Warga RM, Kane DA, Ho RK. Fate mapping embryonic blood in zebrafish: multi- and unpotential lineages are segregated at gastrulation. *Dev Cell*. (2009) 16:744–55. doi: 10.1016/j.devcel.2009.04.007

70. Ottenhoff THM, Verreck FAW, Lichtenauer-Kaligis EGR, Hoeve MA, Sanal O, van Dissel JT. Genetics, cytokines and human infectious disease: lessons from weakly pathogenic mycobacteria and salmonellae. *Nat Genet.* (2002) 32:97–105. doi: 10.1038/ng0902-97
71. Etna MP, Giacomini E, Severa M, Coccia EM. Pro- and anti-inflammatory cytokines in tuberculosis: a two-edged sword in TB pathogenesis. *Semin Immunol.* (2014) 26:543–51. doi: 10.1016/j.smim.2014.09.011
72. Seshadri C, Sedaghat N, Campo M, Peterson G, Wells RD, Olson GS, et al. Transcriptional networks are associated with resistance to *Mycobacterium tuberculosis* infection. *PLoS ONE.* (2017) 12:e0175844. doi: 10.1371/journal.pone.0175844
73. Simmons JD, Stein CM, Seshadri C, Campo M, Alter G, Fortune S, et al. Immunological mechanisms of human resistance to persistent *Mycobacterium tuberculosis* infection. *Nat Rev Immunol.* (2018) 18:575–89. doi: 10.1038/s41577-018-0025-3
74. Wang X, Tang X, Zhou Z, Huang Q. Histone deacetylase 6 inhibitor enhances resistance to *Mycobacterium tuberculosis* infection through innate and adaptive immunity in mice. *Pathog Dis.* (2018) 76:1–8. doi: 10.1093/femspd/fty064
75. Trede NS, Langenau DM, Traver D, Look AT, Zon LI. The use of zebrafish to understand immunity. *Immunity.* (2004) 20:367–79. doi: 10.1016/S1074-7613(04)00084-6
76. Davis JM, Clay H, Lewis JL, Ghori N, Herbomel P, Ramakrishnan L. Real-time visualization of *Mycobacterium*-macrophage interactions leading to initiation of granuloma formation in zebrafish embryos. *Immunity.* (2002) 17:693–702. doi: 10.1016/S1074-7613(02)00475-2
77. Mendez-Samperio P, Trejo A, Miranda E. Activation of ERK1/2 and TNF- α production are mediated by calcium/calmodulin, and PKA signaling pathways during *Mycobacterium bovis* infection. *J Infect.* (2006) 52:147–53. doi: 10.1016/j.jinf.2005.02.027
78. Lee HJ, Ko HJ, Song DK, Jung YJ. Lysophosphatidylcholine promotes phagosome maturation and regulates inflammatory mediator production through the protein kinase A-phosphatidylinositol 3 kinase-p38 mitogen-activated protein kinase signaling pathway during *Mycobacterium tuberculosis* infection in mouse macrophages. *Front Immunol.* (2018) 9:920. doi: 10.3389/fimmu.2018.00920
79. Liu Y, Schneider MF. Opposing HDAC4 nuclear fluxes due to phosphorylation by beta-adrenergic activated protein kinase A or by activity or Epac activated CaMKII in skeletal muscle fibres. *J Physiol.* (2013) 591:3605–23. doi: 10.1113/jphysiol.2013.256263
80. Walkinshaw DR, Weist R, Xiao L, Yan K, Kim G-W, Yang X-J. Dephosphorylation at a conserved SP motif governs cAMP sensitivity and nuclear localization of class IIa histone deacetylases. *J Biol Chem.* (2013) 288:5591–605. doi: 10.1074/jbc.M112.445668
81. Zhu CZ, Cai Y, Zhu JL, Zhang LY, Xing AY, Pan LP, et al. Histone deacetylase inhibitors impair the host immune response against *Mycobacterium tuberculosis* infection. *Tuberculosis.* (2019) 118:101861. doi: 10.1016/j.tube.2019.101861
82. Coussens AK, Wilkinson RJ, Martineau AR. Phenylbutyrate is bacteriostatic against *Mycobacterium tuberculosis* and regulates the macrophage response to infection, synergistically with 25-hydroxy-vitamin D-3. *PLoS Pathog.* (2015) 11:e1005007. doi: 10.1371/journal.ppat.1005007
83. Domingo-Gonzalez R, Prince O, Cooper A, Khader S. Cytokines and chemokines in *Mycobacterium tuberculosis* infection. *Microbiol Spect.* (2016) 4:1–37. doi: 10.1128/microbiolspec.TB2-0018-2016
84. Cui SN, Chen ZY, Yang XB, Chen L, Yang YY, Pan SW, et al. Trichostatin A modulates the macrophage phenotype by enhancing autophagy to reduce inflammation during polymicrobial sepsis. *Int Immunopharmacol.* (2019) 77:105973. doi: 10.1016/j.intimp.2019.105973
85. Songane M, Kleinnijenhuis J, Netea MG, van Crevel R. The role of autophagy in host defence against *Mycobacterium tuberculosis* infection. *Tuberculosis.* (2012) 92:388–96. doi: 10.1016/j.tube.2012.05.004
86. Clocchiatti A, Di Giorgio E, Ingrao S, Meyer-Almes FJ, Tripodo C, Brancolini C. Class IIa HDACs repressive activities on MEF2-dependent transcription are associated with poor prognosis of ER(+) breast tumors. *FASEB J.* (2013) 27:942–54. doi: 10.1096/fj.12-209346
87. Koenis DS, Medzikovic L, van Loenen PB, van Weeghel M, Huvencers S, Vos M, et al. Nuclear receptor Nur77 limits the macrophage inflammatory response through transcriptional reprogramming of mitochondrial metabolism. *Cell Rep.* (2018) 24:2127–40.e2127. doi: 10.1016/j.celrep.2018.07.065
88. Hamers AA, Vos M, Rassam F, Marinkovic G, Kurakula K, van Gorp PJ, et al. Bone marrow-specific deficiency of nuclear receptor Nur77 enhances atherosclerosis. *Circ Res.* (2012) 110:428–38. doi: 10.1161/CIRCRESAHA.111.260760
89. Hanna RN, Shaked I, Hubbeling HG, Punt JA, Wu R, Herrley E, et al. NR4A1 (Nur77) deletion polarizes macrophages toward an inflammatory phenotype and increases atherosclerosis. *Circ Res.* (2012) 110:416–27. doi: 10.1161/CIRCRESAHA.111.253377
90. Gregoire S, Yang XJ. Association with class IIa histone deacetylases upregulates the sumoylation of MEF2 transcription factors. *Mol Cell Biol.* (2005) 25:2273–87. doi: 10.1128/MCB.25.6.2273-2287.2005
91. Gregoire S, Tremblay AM, Xiao L, Yang Q, Ma K, Nie J, et al. Control of MEF2 transcriptional activity by coordinated phosphorylation and sumoylation. *J Biol Chem.* (2006) 281:4423–33. doi: 10.1074/jbc.M509471200

Conflict of Interest: The authors declare that the research was conducted in the absence of any commercial or financial relationships that could be construed as a potential conflict of interest.

Copyright © 2020 Moreira, Koch, van Veen, Walburg, Vrieling, Mara Pinto Dabés Guimarães, Meijer, Spaink, Ottenhoff, Haks and Heemskerk. This is an open-access article distributed under the terms of the Creative Commons Attribution License (CC BY). The use, distribution or reproduction in other forums is permitted, provided the original author(s) and the copyright owner(s) are credited and that the original publication in this journal is cited, in accordance with accepted academic practice. No use, distribution or reproduction is permitted which does not comply with these terms.